SECONDARY HARDENING IN 2090 (Al-Cu-Li) ALLOY

X. GAO, J.F. NIE and B.C. MUDDLE
Department of Materials Engineering, Monash University, Clayton, Victoria 3168, Australia

ABSTRACT A study has been made of secondary precipitation hardening behaviour and the accompanying microstructural changes in alloy 2090. The alloy samples were typically aged initially to maximum hardness at 200°C and then subjected to longer term isothermal ageing (≤2400h) over a range of lower temperatures (90-150°C). Such treatments have demonstrated the existence of a significant secondary hardening phenomenon during the low temperature exposure (90-130°C) in alloy 2090, and the corresponding increase in yield strength is accompanied by a significant reduction in toughness. The secondary hardening observed at 90°C is mainly attributable to the formation of Guinier-Preston (GP) zones, while that occurring at 130°C is associated with the precipitation of θ" and θ' phases. Such secondary precipitation implies the existence of a residual excess of solute Cu in solid solution in samples aged to maximum strength at the upper ageing temperature.

Keywords: *precipitation hardening, secondary hardening, Al-Cu-Li alloys, alloy 2090.*

1. INTRODUCTION

Most notable in the development of high-strength aluminium alloys for use in the aircraft and aerospace industries are the Li-modified Al-Cu alloys, such as those designated 2090 (Al-Cu-Li), 8090 (Al-Li-Cu-Mg) [1], and the Weldalite™ series of 2095 (Al-Cu-Li-Mg-Ag) [2]. The presence of lithium as a major alloying element leads to a significant simultaneous reduction in density and increase in stiffness and strength, with tensile yield strengths in the range 500-750 MPa achievable through precipitation strengthening. However, despite the potential advantages of these Al-Cu-Li alloys, their adoption in practical applications has remained limited. There are a variety of reasons for this [3, 4], with a deterioration in toughness during low temperature (~70°C) thermal exposure one of the more significant problems. Aside from these well-recognised problems, there is also evidence that the microstructures and hence mechanical properties of these alloys have yet to be optimised. It has been demonstrated, for example, that there is a potential for a secondary hardening phenomenon in alloy 2090, aged initially to maximum hardness at 150-160°C and then exposed for an extended period at 70-120°C [5-7]. The corresponding increase in yield strength is accompanied by a significant reduction in toughness in extruded product. The existence of this secondary hardening, and the associated lack of thermal stability at low temperatures, suggest a need for revision of heat treatment schedules currently adopted for this alloy. The present work involves a systematic re-examination of secondary precipitation hardening behaviour in alloy 2090.

2. EXPERIMENTAL PROCEDURE

An alloy 2090 with a composition of Al-2.86Cu-2.05Li-0.12Zr (wt.%) was provided by COMALCO Australia. The alloy was homogenised, scalped and hot rolled to ~5mm strip for bulk Vickers hardness testing (5kg load), and to sheet ~0.5mm thick for preparation of electron microscope thin foils. Samples were solution treated 1h at 540°C in a salt bath, cold water quenched, and initially aged to maximum hardness in a salt bath at 200°C for 12h. They were then subjected to long term isothermal ageing in oil baths at 90, 130 and 150°C. Discs 3mm in diameter were punched from heat-treated sheets, and specimens for transmission electron microscopy (TEM) were prepared by twin-jet electropolishing in a solution of 33 vol.% nitric acid and 67 vol.% methanol, at -25°C and 12V. The microstructures were examined in a Philips CM20 transmission electron microscope (200 keV).

3. RESULTS

3.1 Secondary Hardening Response

Figure 1 illustrates the hardness changes in samples of the alloy 2090 aged 12h at 200°C to maximum hardness (~150 VHN) and then subjected to second stage ageing at 90°C, 130°C and 150°C. It confirms clearly the existence of a significant secondary hardening phenomenon during exposure at both 90°C and 130°C, with the hardness increasing from ~150 VHN to 167 VHN and 161 VHN after ageing 2400h at 90°C and 130°C respectively. In contrast, there was no secondary hardening of the alloy during further ageing at 150°C. The hardness decreased gradually with progress of the secondary ageing at 150°C, with almost the same pattern as that observed in the overageing stages when the alloy was aged isothermally at 150°C.

It is also noticeable that there was an initial incubation period in excess of 48h, during the low temperature exposures at 90°C and 130°C, before any significant secondary hardening effect was detectable. The rate of secondary hardening in the early stages of ageing (<480h) was more rapid at 130°C than at 90°C. However, with further increase in ageing time, the level of the hardening response at 90°C began to exceed that at 130°C. The maximum hardness increment in this temperature range corresponds to an approximately 10% increase on the maximum hardness achievable during the preliminary hardening at the temperature of 200°C.

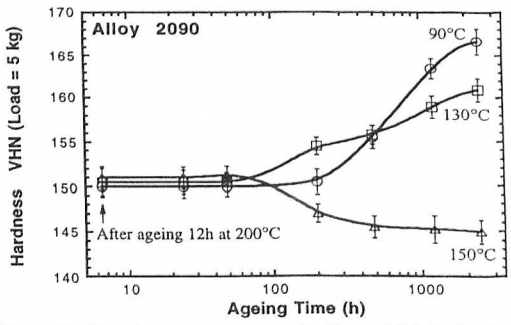

Fig. 1 Hardness curves of alloy 2090 during secondary ageing at 90, 130 and 150°C, after initial ageing at 200°C for 12h.

3.2 Microstructural Changes

Initial Ageing to Maximum Hardness at 200°C

Figures 2(a) and (b) show $<100>_\alpha$ and $<110>_\alpha$ bright-field (BF) TEM micrographs, together with the corresponding selected area electron diffraction (SAED) patterns, representative of the microstructure of the alloy after ageing 12h at 200°C. The microstructure contained predominantly plate-shaped $\{111\}_\alpha$ T_1 (Al_2CuLi) precipitates, a uniform dispersion of coherent ordered δ' (Al_3Li) phase, a small fraction of $\{001\}_\alpha$ θ' (Al_2Cu) plates, and minor portions of T_B ($Al_{7.5}Cu_4Li$) phase and β' (Al_3Zr) dispersoids; all distributed within the α matrix. A few T_2 (Al_6CuLi_3) phase precipitates were detectable on high angle grain boundaries. In any $<100>_\alpha$ orientation, Fig. 2(a), two sets of $\{001\}_\alpha$ θ' plates were observed lying parallel to the incident electron beam, *i.e.* edge-on, while the $\{111\}_\alpha$ T_1 plates were inclined to the electron beam. In the $<110>_\alpha$ orientation, Fig. 2(b), two variants of $\{111\}_\alpha$ T_1 plates and one set of $\{001\}_\alpha$ θ' plates were observable lying edge-on, while other variants of the T_1 and θ' particles were inclined to the electron beam and revealed by patches of weak fringe contrast. The spheroidal δ' particles were distributed uniformly within the α matrix. It was also noticeable that the broad faces of the θ' plates were coated with coherent δ', and that the θ' plates remained, as a result, extremely thin and of high aspect ratio. It appeared that the coverage of δ' phase on the broad faces of the θ' plates restricted growth in the thickness of the θ' phase in this alloy, perhaps by restricting access of Cu atoms to the broad faces of the plates and normal ledge-wise growth.

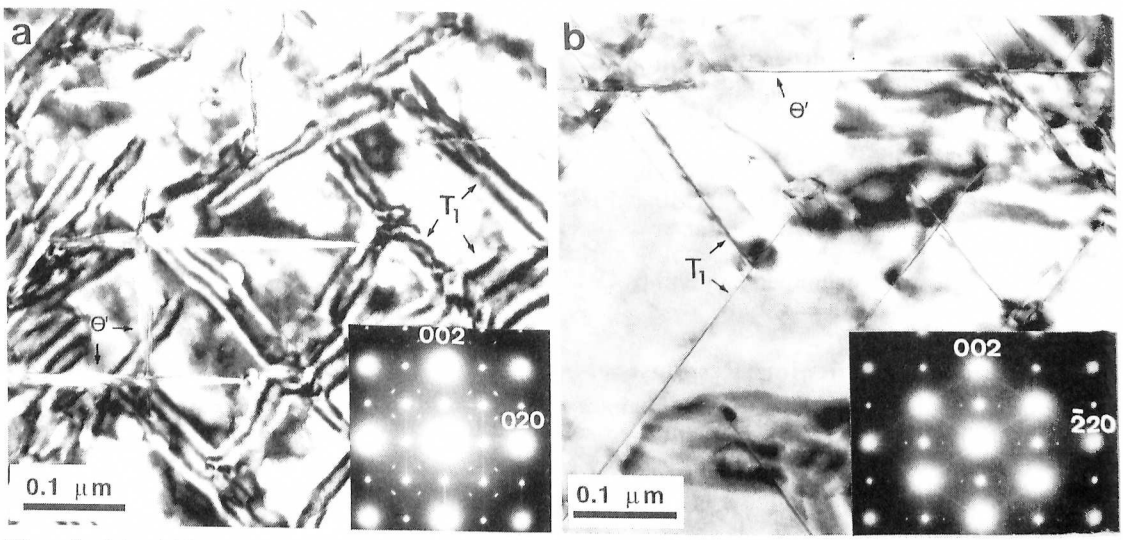

Fig. 2 (a) $<100>_\alpha$, and (b) $<110>_\alpha$ BF TEM micrographs, together with the corresponding SAED patterns, showing microstructure of the alloy aged to maximum hardness at 200°C for 12h.

Aside from the direct microstructural observations, the identification of the major phases was also supported by the corresponding SAED patterns. Those reflections located at 1/3 and 2/3$\{022\}_\alpha$, Figs. 2(a) and (b), together with the streaks in the $<111>_\alpha$ directions, Fig. 2(b), are attributable to the hexagonal T_1 (a = 0.497 nm, c = 0.934 nm) phase, while the superlattice reflections at 1/2$\{002\}_\alpha$ and 1/2$\{022\}_\alpha$, Figs. 2(a) and (b), arise primarily from the $L1_2$ δ' phase, with a minor contribution from the β' phase. The intensity maxima near 2/3$\{002\}_\alpha$ positions are characteristic of the tetragonal θ' (a = 0.404 nm, c = 0.580 nm) phase.

Secondary Ageing at 90°C

Figures 3(a) and (b) show $<100>_\alpha$ BF TEM micrographs, together with the corresponding SAED patterns, representative of the microstructure of the alloy after secondary ageing at 90°C for 480 and 2400h respectively. After 480h, Fig. 3(a), it was revealed that, in addition to those previously precipitated phases shown in Fig. 2, there was a significant fraction of fine-scale Guinier-Preston (GP) zones formed on the $\{001\}_\alpha$ planes. These newly-formed GP zones were distributed principally within those regions of matrix α containing little or no T_1 and θ' precipitation, while the region occupied by and surrounding clusters of T_1 and/or θ' precipitates were free of secondary precipitation. The corresponding SAED pattern, Fig. 3(a), shows the continuous streaks of weak, diffuse intensity along $<001>_\alpha$ directions that are the sole diffraction feature typical of the GP zones. On further ageing to approximately 2400h, significant increases in the size and volume fraction of the precipitated GP zones were observed, Fig. 3(b), along with an increase in the intensity of the streaking attributable to the GP zones in the corresponding SAED pattern. Apart from the presence of these 'secondary' GP zones, no other changes were detectable in the precipitate microstructures of those samples aged at 90°C for up to 2400h.

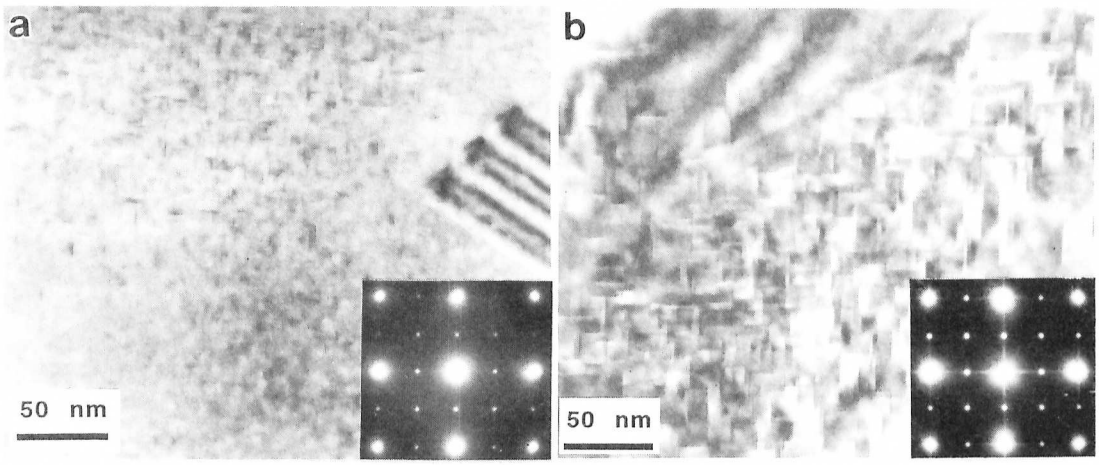

Fig. 3 $<100>_\alpha$ BF TEM micrographs, together with the corresponding SAED patterns, showing the microstructure of the alloy after secondary ageing at 90°C for (a) 480h and (b) 2400h.

Secondary Ageing at 130°C

Figures 4(a) and (b) compare $<100>_\alpha$ BF TEM micrographs, and the corresponding SAED patterns, recorded from alloy samples after secondary ageing at 130°C for 240 and 2400h respectively. In contrast to observations following ageing at 90°C, the GP zones were not detectable at this ageing temperature. The new microstructural constituent in samples aged 240h at 130°C took the form of fine, plate-shaped θ" phase lying on the $\{001\}_\alpha$ planes and again located within those volumes of matrix α containing little or no T_1 and/or θ', Fig. 4(a). The corresponding SAED pattern shows the discontinuous, diffuse streaks, adjacent to the $\{001\}_\alpha$ reflections and extending along the $<001>_\alpha$ directions, that are considered the diffraction feature typical of θ" phase [8]. The θ" precipitates coarsen and increase in volume fraction during further ageing, and the microstructure of the alloy aged to 2400h at 130°C, Fig. 4(b), contained a mixture of residual θ" and some newly-formed θ' phase in matrix regions typical of those where only 'secondary' θ" had previously formed. At this stage of ageing, some θ" plates have been replaced by θ' precipitates.

It was noticeable that the size of these newly-formed θ' plates was significantly smaller than that of θ' formed after the initial ageing treatment to maximum hardness at 200°C . Moreover, there was no obvious sign that those θ' precipitates, formed during the initial ageing treatment at 200°C, were under-going re-solution during the long term secondary ageing (2400h) at both 90 and 130°C.

Observations of the microstructures arising from short term secondary ageing (≤ 48h) treatments at both 90 and 130°C revealed no evidence of precipitation of either GP zones or θ'' phase. However, there was very weak, diffuse $<001>_\alpha$ streaking evident in $<100>_\alpha$ electron diffraction patterns consistent with clustering on $\{001\}_\alpha$ planes after ageing for ~120h at 130°C.

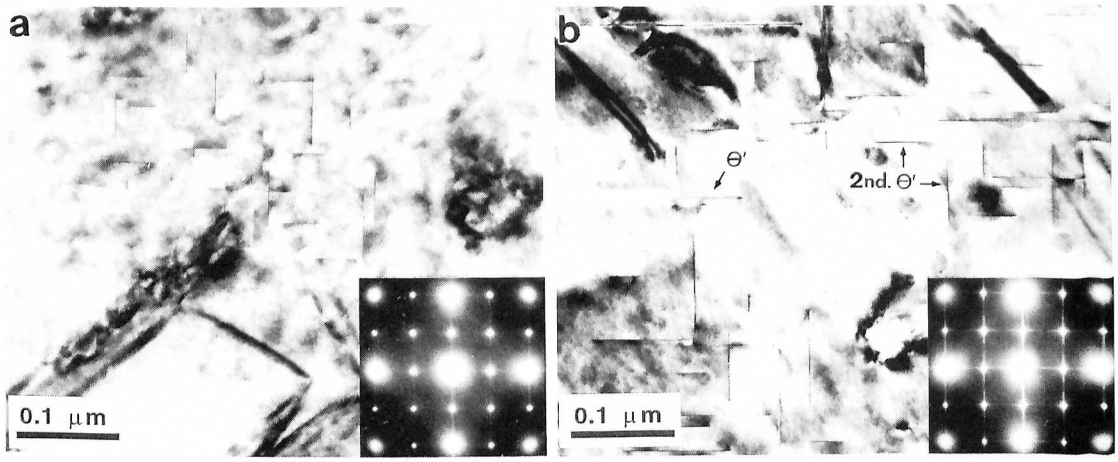

Fig. 4 $<100>_\alpha$ BF TEM micrographs, together with the corresponding SAED patterns, showing the microstructure of the alloy after secondary ageing at 130°C for (a) 480h and (b) 2400h.

Secondary Ageing at 150°C

In contrast to observations following ageing at 90 and 130°C, there was no evidence of any new precipitation reaction during the secondary ageing treatment at 150°C. Figure 5 presents a $<100>_\alpha$ BF TEM micrograph, together with the corresponding SAED pattern, representative of a sample after secondary ageing at 150°C for 2400h. As with the initial microstructure arising from ageing for 12h at 200°C, Fig. 2, the microstructure shown in Fig. 5 contained only those precipitate phases formed during the initial treatment, *i.e.* T_1, δ', θ', T_B, T_2 and β'. The corresponding $<100>_\alpha$ SAED pattern is identical to that shown in Fig. 2(a). It was, however, clearly evident that the primary strengthening phases T_1, δ' and θ' had all coarsened during the additional ageing treatment of 2400h at 150°C, offering a plausible explanation for the decrease in hardness that accompanies secondary ageing at this temperature.

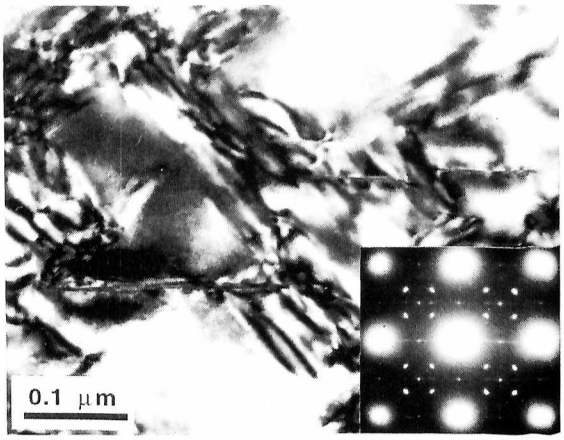

Fig. 5 $<100>_\alpha$ BF TEM micrograph and the corresponding SAED pattern, showing the microstructure after secondary ageing at 150°C for 2400h.

4. DISCUSSION

The present results confirm the existence of a secondary hardening phenomenon in alloy 2090, aged initially to maximum hardness at 200°C and then exposed for an extended period at 90 or 130°C. A similar effect has previously been reported [5-7] and suggested to be responsible for the increase in strength and decrease in toughness that accompany lower temperature (70-120°C) thermal exposure of

strength and decrease in toughness that accompany lower temperature (70-120°C) thermal exposure of the alloy initially aged to maximum hardness at 150-160°C. In the present study, it was observed that the secondary hardening occurring during the low temperature exposure at 90°C is attributable to the slow formation of GP zones, while that at 130°C is due to, at least in part, the precipitation of θ" and θ' phases. A similar result has been observed in alloy 2090 aged at 120°C and attributed to coarsening of the δ' dispersion and an increase in the order hardening increment [6], and such a contribution to secondary hardening cannot be ruled out in the present work. In contrast to the behaviour at 90 and 130°C, there was no secondary hardening observable during the heat treatment at 150°C, which is consistent with failure to detect any new precipitation at this ageing temperature. The coarsening of the existing precipitates, formed during the initial ageing treatment of 12h at 200°C, seems likely to contribute to the gradual decrease in hardness with the progress of secondary ageing at 150°C.

The precipitation sequence observed within local regions of α matrix during secondary ageing of alloy 2090 in the range 90-130°C is similar to that in binary Al-Cu alloys, in which the intermediate GP zones, θ" and θ' form in order with increasing time at a temperature below the coherent GP zone solvus, and in which each in turn becomes the preferred intermediate phase with increasing ageing temperature [9]. This implies that there is a local residual excess of Cu retained in the solid solution α matrix, even after the alloy has been aged to maximum hardness at 200°C. The present observations indicate that, for solid solution with this residual Cu content the coherent solvus is above 90°C but below 130°C, while the solvus temperature for θ" is above 130°C but below 150°C. Based on previously reported solvus temperatures for the GP zones and θ" phase in binary Al-Cu alloys [10, 11], it may be estimated from the observation of the presence of the GP zones during ageing at 90°C and the θ" at 130°C, together with the absence of both intermediate phases at 150°C, that the retained Cu concentration within the matrix may be as high as 1 wt%,. This is regardless of any retardation in the formation of GP zones due to the presence of Li [12]. It is most likely that such a significant concentration of residual Cu within the α matrix phase, even after the alloy has been initially aged to maximum hardness at an elevated temperature, is the result of incomplete precipitation of the Cu-containing precipitates T_1 and θ'.

It should be noted that the lack of sufficient precipitation of the Cu-containing T_1 and θ' phases cannot simply be attributed to the absence of a deformation step during the heat treatment schedule of the present alloy. Deformation prior to ageing is commonly employed with such alloys to encourage a uniform distribution of dislocations that facilitate the nucleation of both T_1 and θ' precipitates. It has been shown, however, that there is still a secondary hardening phenomenon attributable to the precipitation of GP zones in alloy 2090 during low temperature (70°C) exposure, even when the alloy is stretched 4-6% prior to the initial ageing [5].

Tosten *et al.* [13] have found that a decrease in the volume fractions of both the δ' and θ' phases, and a concomitant increase in the volume fraction of the T_1 precipitate, occur during overageing (540h at 190°C) of the alloy 2090. As a consequence, they proposed that the δ' and θ' phases dissolve to provide solute Li and Cu for the subsequent formation of T_1 precipitate in the overaged condition. However, this was not observed in the present study for secondary ageing treatments of up to 2400h at 90 and 130°C. In addition, it has been suggested that, after long term ageing at elevated temperatures, the θ' precipitate may transform into the T_B phase in Al-Cu-Li alloys by the incorporation of Li in the θ' lattice [14, 15]. Therefore, it is not feasible that the Cu atoms available for the formation of GP zones, θ" or θ' within the α matrix phase during low temperature secondary ageing arise from the dissolution of the θ'. The θ' is after all a more stable phase thermodynamically.

A low supersaturation of retained Cu solute in the α matrix, the absence of excess 'quenched-in' vacancies and the lower ageing temperatures, are all factors likely to contribute to the incubation period (~48h) observed during the secondary ageing treatments and to the sluggish precipitation kinetics at 90 and 130°C. That the onset of the θ" precipitation in the alloy during thermal exposure at 130°C is faster than that of GP zones at 90°C is contrary to conventional experience in quenched and aged Al-Cu alloys, and probably simply attributable to the fact that the atomic diffusivity for solute Cu increases with the increasing temperature. This results in the secondary hardening response being comparatively stronger in the early stages of ageing (480h) at 130°C. However, continued ageing at 90°C produces a more refined, denser dispersion of GP zones, which is ultimately responsible for a significantly increased hardening response. In contrast, for samples aged long term at 130°C, the θ" coarsens and is then replaced by θ' precipitates in a relatively coarse form. Those existing precipitates, formed during the initial ageing treatment at 200°C, may also coarsened more rapidly during exposure at 130°C than at 90°C. In consequence, the total hardening effect for the alloy during

long-term secondary ageing at 130°C is expected to be smaller than that at 90°C.

Aside from accounting for the changes in mechanical properties accompanying low temperature exposure, the occurrence of secondary hardening suggests that the common heat treatment schedules employed with alloy 2090 and the mechanical properties obtained, are far from optimised. Approaches to promoting the nucleation and growth of the effective intermediate strengthening phases, T_1 and θ', remain possible to maximise the strength and hardness. An examination of the potential to use modified heat treatments and/or microalloying additions to improve significantly the microstructural design, and hence to optimise the combination of strength and toughness of the alloy, will be an objective of future study.

5. SUMMARY

A systematic study of precipitation hardening behaviour and accompanying microstructural changes in alloy 2090, aged initially to maximum hardness at temperature 200°C and then subjected to long term isothermal ageing over a range of lower temperatures (90-150°C), has confirmed the existence of significant secondary hardening during exposure at temperature up to 130°C. It has been found that: (i) the secondary hardening observed at temperatures up to 90°C is mainly attributable to the diffusion-controlled formation of Guinier-Preston (GP) zones, (ii) the hardening at 130°C is, in contrast, at least partially the result of precipitation of θ" and θ' phases, and (iii) there is no secondary hardening phenomenon during heat treatment at 150°C. These observations imply the existence of a residual excess of solute Cu in solid solution in samples aged to peak hardness at temperatures of 150-200°C. This excess is confined to those regions free of Cu-containing intermediate precipitate phases T_1 and θ'. Within such regions of solid solution, the Cu concentration is such that the effective coherent solvus temperature exceeds 90°C but is below 130°C. The corresponding solvus temperature for θ" is above 130°C but below 150°C.

ACKNOWLEDGMENTS

The authors acknowledge gratefully the support of the Australian Research Council.

REFERENCES

[1] E.A. Starke Jr.: *'Aluminum Alloys - Contemporary Research and Applications'*, Treatise on Materials Science and Technology, (A.K. Vasudevan and R.D. Doherty, eds.), Academic Press, 31(1989), 35.

[2] I.R. Pickens, F.H. Heubaum, T.J. Langan and L.S. Kramer: *Proc. 5th Int. Conf. on Aluminium-Lithium Alloys*, (E.A. Starke Jr. and T.H. Sanders Jr., eds.), Mat. and Comp. Eng. Publications, Birmingham, U.K., (1989), 1397.

[3] S.P. Lynch: *Mater. Sci. Eng.*, A136(1991), 25.

[4] E.S. Balmuth and D.J. Chellman: *Proc. 4th Int. Conf. on Aluminum Alloys (ICAA-4)*, (T.H. Sanders and E.A. Starke Jr., eds.), The Georgia Inst. of Tech., Atlanta, GA, (1994), 282.

[5] B.C. Muddle, E.D. Sweet, M.J. Kerr and C.G. Bennett: *Metall. Mater. Trans. A*, submitted for publication (1998).

[6] A.J. Weber, D.J. Chellman and A.J. Ardell: *'Advanced Aluminum and Magnesium Alloys (Proc. Conf.)'*, ASM International Materials Park, Ohio 44073, USA, (1990), 51.

[7] B. Noble, S.J. Harris and K. Dinsdale: *Proc. 4th Int. Conf. on Aluminum Alloys (ICAA-4)*, (T.H. Sanders and E.A. Starke Jr., eds.), The Georgia Inst. of Tech., Atlanta, GA, (1994), 460.

[8] V.A. Philips: *Acta Metall.*, 23(1975), 751.

[9] J.M. Silcock, T.J. Heal and H.K. Hardy: *J. Inst. Metals*, 82(1953-54), 239.

[10] R.H. Beton and E.C. Rollason: *J. Inst. Metals*, 86(1957-58), 77.

[11] E. Hornbogen: *Aluminium*, 43(1967), 9.

[12] H.-H. Jo and K. Hirano: *Mater. Sci. Forum*, 13/14(1987), 377.

[13] M.H. Tosten, A.K. Vasudevan and P.R. Howell: *Metall. Trans. A*, 19A(1988), 51.

[14] K. Schneider and M. von Heimendahl: *Z. Metallkde*, 64(1973), 342.

[15] Y.-S. Lee: *Ph.D Thesis*, Monash University, Australia, (1996).